

Journal of Materials Chemistry A

Accepted Manuscript



This is an *Accepted Manuscript*, which has been through the Royal Society of Chemistry peer review process and has been accepted for publication.

Accepted Manuscripts are published online shortly after acceptance, before technical editing, formatting and proof reading. Using this free service, authors can make their results available to the community, in citable form, before we publish the edited article. We will replace this *Accepted Manuscript* with the edited and formatted *Advance Article* as soon as it is available.

You can find more information about *Accepted Manuscripts* in the [Information for Authors](#).

Please note that technical editing may introduce minor changes to the text and/or graphics, which may alter content. The journal's standard [Terms & Conditions](#) and the [Ethical guidelines](#) still apply. In no event shall the Royal Society of Chemistry be held responsible for any errors or omissions in this *Accepted Manuscript* or any consequences arising from the use of any information it contains.



Highly stable hollow bifunctional cobalt sulfides for flexible supercapacitor and hydrogen evolution

C. Ranaveera^a, Z. Wang^a, E. Alqurashi^a, P. K. Kahol^b, P. Dvornic^a, Bipin Kumar Gupta^c, Karthik Ramasamy^d, Aditya D. Mohite^e, Gautam Gupta^e and Ram K. Gupta^{*a}

Received 00th January 20xx,
Accepted 00th January 20xx

DOI: 10.1039/x0xx00000x

www.rsc.org/MaterialsA

Hollow structures of NiAs-type cobalt sulfide have been synthesized by a facile hydrothermal method. These hollow structured cobalt sulfides exhibit excellent electrochemical properties for supercapacitor applications (867 F/g) and respectable hydrogen evolution activity. The symmetrical supercapacitor device fabricated using cobalt sulfide nanostructure showed areal capacitance of 260 mF/cm² with good flexibility and high temperature stability. Specific capacitance of the supercapacitor is enhanced over 150 %, when the temperature is raised from 10 to 70 °C.

Over the last few decades, the increasing demand for the energy motivated the scientific community to develop high performance, sustainable, cost-effective and environmentally friendly materials for energy conversion and storage applications¹⁻⁴. Undoubtedly, materials for supercapacitors and hydrogen evolution are among the widely studied ones for these purposes. Supercapacitors are electrochemical energy storage devices primarily appealed for their excellent power density and long cycle life⁴⁻⁷. Carbon based electrodes are suitable for delivering the high power density but have low energy density⁸. Nevertheless, in recent years the energy density of supercapacitors has been boosted by the use of metal oxides, which in turn sacrifices the cycle life⁴.

Second, energy generation using a cleaner and cheaper method is of high importance due to increasing concerns of carbon emission. Hydrogen generation by splitting water is highly desired. Hydrogen evolution reaction (HER) is one of the key steps in water splitting process⁹. Ideally, the thermodynamic potential for hydrogen evolution reaction should be at 0 V (vs. SHE). However, without an efficient catalyst, this reaction occurs at high overpotential¹⁰.

Presently, platinum is the most effective and durable catalyst for hydrogen evolution reaction, but its wide spread use is precluded due to its high cost and limited availability.

At this juncture it is essential to develop cost effective, sustainable and stable materials for both supercapacitor and HER applications. Recently, transition metal chalcogenides have attracted considerable attention for energy applications such as fuel cells, supercapacitors and batteries due to their high abundance, low cost and decent performance^{2, 11-15}. Wang *et al* have synthesized 3D flower-like MoS₂ nanostructures and were used as an electrode for high-performance electrochemical capacitors¹⁶. The MoS₂ electrode showed a specific capacitance of 168 F/g and retained 92.6% of capacitance even after 3,000 cycles. Soon *et al* have reported a MoS₂ based supercapacitor having a capacitance of 8 mF/cm²¹⁷. Hierarchically porous nickel sulfide has been synthesized for both HER and oxygen evolution reaction (OER)¹⁸. The synthesized nickel sulfide showed overpotentials of 60 mV for HER and 180 mV for OER in 1.0 M KOH at a current density of 10 mA/cm², respectively. Sharma *et al* have synthesised flower like ZnS for charge storage application¹⁹. They observed a high specific capacitance (226 F/g) and specific capacitance was observed to decrease by 60 % on increasing the scan rate from 20 to 200 mV/s. Other metal sulfide such as WS₂ is also synthesized for HER, supercapacitors and batteries applications²⁰⁻²². As an important member of the transition metal sulfide family, cobalt sulfide is considered to be one of the promising candidates for such applications. Accordingly, various phases of cobalt sulfides have been synthesized and studied for supercapacitor and HER applications^{23,24-29}.

Xing *et al* have synthesized octahedron-shaped CoS₂ crystals using a hydrothermal method for their application in supercapacitors³⁰. These CoS₂ crystals showed a specific capacitance of 237 F/g at 1 A/g with only a loss of 7.4% in the specific capacitance after 2000 cycles. Sphere like CoS nanostructures were synthesized and used as an electrode material for charge storage applications³¹. These sphere like CoS showed very stable electrochemical performance with only about 13% reduction in charge storage capacity of the available capacitance (363 F/g) on increasing the scan rate by 10 times. Ray *et al* have used a facile electrochemical technique to fabricate titania nanotube-CoS composite electrode for supercapacitor applications³². Cyclic voltammetric measurements presented a very high specific capacitance (370 F/g) with great cycle stability in KOH electrolyte. Since various phases of cobalt sulfides

^a Department of Chemistry, Pittsburg State University, 1701 S. Broadway, Pittsburg, KS 66762, USA, E-mail: ramguptamsu@gmail.com

^b Department of Physics, Pittsburg State University, 1701 S. Broadway, Pittsburg, KS 66762, USA, E-mail: ramguptamsu@gmail.com

^c National Physical Laboratory (CSIR), Dr K.S. Krishnan Road, New Delhi 110012, India

^d Center for Integrated Nanotechnologies, Los Alamos National Laboratory, Albuquerque, NM-87185, USA

^e Materials Physics and Application Division, Los Alamos National Laboratory, Los Alamos, NM-87545, USA

Electronic Supplementary Information (ESI) available: [synthesis, characterization and some additional figures]. See DOI: 10.1039/x0xx00000x

COMMUNICATION

have been found useful for energy storage and catalytic applications, it is highly desirable to synthesize cobalt sulfide using a facile and efficient method to explore its multifunctionality. Herein, we report a facile one step hydrothermal synthesis of hollow structured NiAs type cobalt sulfide and investigate the material for supercapacitor and HER applications. Our investigations show excellent electrochemical properties for supercapacitor applications with a specific capacitance of 867 F/g and an electrocatalyst for hydrogen evolution reaction (Tafel slope of 97 mV/decade). The high performance of the cobalt sulfide could be due to the unique morphology.

Hollow structured cobalt sulfide was synthesized by reacting cobalt nitrate with thioacetamide in ethylene glycol under a hydrothermal condition at 180 °C for 12 h (details in ESI). Powder XRD pattern of the black precipitate from the hydrothermal reaction showed diffraction planes, predominantly matching with NiAs-type hexagonal Co_{1-x}S phase of cobalt sulfide (JCPDS file: 42-0826). The diffraction peaks can be indexed to the (010), (011), (012), (120) planes of Co_{1-x}S (Fig. 1a). Scanning electron microscope image of the cobalt sulfide obtained by a hydrothermal reaction exhibited irregular shaped granules (Fig. 1b). The ratio of cobalt to sulfur determined from SEM-EDX was found to be 0.98, close to the expected composition for Co_{1-x}S (Fig. 1S, ESI). To gain morphological insight, TEM imaging was performed. TEM image in Fig. 1c shows nearly uniform hollow ring like structures that are composed of pseudo-spherical nanocrystals. It is widely accepted that the hollow structures are consequence of difference in diffusion rates of constituent elements³³. A similar hollow structure has also been reported by microwave assisted synthesis of cobalt sulfide³³. Lattice distance measured from HRTEM image (Fig. 1d) of Co_{1-x}S nanocrystals was close to 0.293 nm corresponding to (010) plane. In addition, we have carried out BET nitrogen adsorption/desorption isotherm measurements to determine the surface area of the sample (Fig. 2S, ESI). The hysteresis loop in the isotherm of the synthesized Co_{1-x}S is the indication of capillary condensation, which arises due to different mechanisms of adsorption/desorption in micropores. The synthesized Co_{1-x}S showed a specific surface area of 23.9 m²/g which

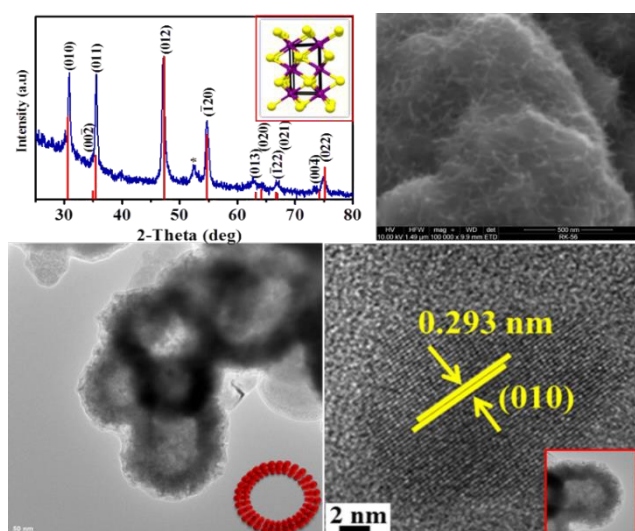


Fig. 1: (a) XRD pattern (Inset: crystals structure of Co_{1-x}S), (b) SEM image, (c) TEM image (Inset: Schematic of hollow structure composed of nanocrystals), and (d) HRTEM image of synthesized cobalt sulfide (inset: Low magnification TEM image of hollow structure).

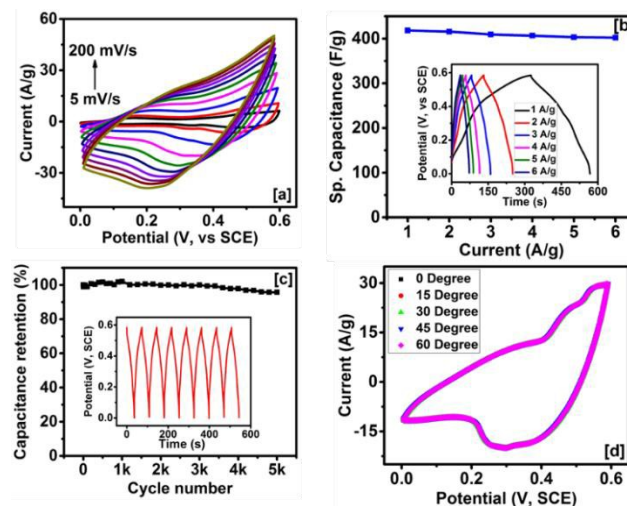
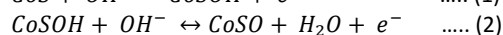
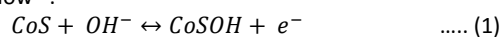


Fig. 2 (a) CV curves at various scan rates, (b) variation of specific capacitance with applied current (inset figure show potential-time curves at different applied currents), (c) capacitance retention as a function of number of charge-discharge cycles (inset figure shows first few cycles of charge-discharge curves), and (d) CV curves at various bending angles of cobalt sulfide electrode.

is much higher than commercial samples of CoS (0.39 m²/g and MoS₂ (3.33 m²/g).

The electrochemical properties of electrode prepared using Co_{1-x}S hollow structures were studied using cyclic voltammetry (CV), galvanostatic charge-discharge (GCD), and electrochemical impedance spectroscopy (EIS). The CV measurements of Co_{1-x}S electrode in alkaline electrolyte (3M NaOH) displayed non-rectangular shape curves with quasi-reversible redox waves in potential range of 0 to 0.6 V (Fig. 2a). The unambiguous appearance of redox waves, confirms the pseudocapacitive behaviour of Co_{1-x}S . As evident, the charge-storage mechanism in CoS is significantly Faradic in nature than capacitive type. The Faradic reaction occurring on the surface of CoS electrode in alkaline media is given below³¹:



The specific capacitance of Co_{1-x}S electrode estimated from CV curves was found to be 867 F/g at 5 mV/s (Fig. 3S, ESI). Further, GCD measurements exhibit symmetrical and non-linear charge-discharge characteristics, confirming the pseudocapacitance behaviour of the electrode (inset of Fig. 2b). The specific capacitance of cobalt sulfide electrode determined from GCD measurements is about 420 F/g at 1 A/g, which is significantly higher than the value obtained for CoS hollow nanosheets and hollow nanoprisms^{31, 33}. Interestingly, the specific capacitance value was nearly retained (402 F/g at 6 A/g) even at higher current density (Fig. 2b), suggesting excellent rate stability of Co_{1-x}S hollow structures. In addition, we have evaluated the cyclic stability of the cobalt sulfide electrode using GCD measurements. From Fig. 2c, it can be witnessed that the specific capacitance was almost preserved even after 5,000 charge-discharge cycles, confirming their high electrochemical stability. It is noteworthy that electrode using CoS₂ ellipsoids lost nearly 50 % of specific capacitance within 1,000 charge-discharge cycles³⁴. Furthermore, we have tested the flexibility of the cobalt sulfide electrodes by carrying out CV measurements at different bending angles. The shape and size of the CV curves were found to be identical at different bending angles (Fig. 2d), suggesting that Co_{1-x}S hollow structures are exceptional candidates for flexible energy storage devices. The

variation of the specific energy density versus power density (Ragone plot) for cobalt sulfide is shown in Fig. 4S, (ESI). The highest specific energy density of 19.4 Wh/kg and power density of 2644 W/kg was observed.

We fabricated the supercapacitor device by sandwiching an ion transporting layer between two cobalt sulfide electrodes (inset of Fig. 3b). Fig. 3a shows the CV curves of the supercapacitor device at different scan rates. The shape of the voltammogram at various scan rates are similar in nature, suggesting high charge transfer stability of the device even at high scan rates. The near rectangular shape of the CV curves indicates a near ideal capacitive behaviour. The variation of specific capacitance as a function of scan rate for the device is shown in Fig. 3b. The specific capacitance of the device was observed to decrease with increase in the scan rate. The highest areal capacitance of 261 mF/cm² was observed at a scan rate of 5 mV/s. It was observed that specific capacitance of the devices decreases with increasing scan rate, which is due to insufficient time for the electrolyte to form an electrochemical double layer capacitor at cobalt sulfide electrode. The galvanostatic charge-discharge measurements were also performed to study the charge storage capacity of the device. The charge storage capacity of the device decreases with increasing current density (Fig. 5S, ESI). A specific capacitance of 60 mF/cm² was observed at 2 mA/cm² of current density. Further, the effect of temperature on the performance of the supercapacitor device was studied. The CV curves of the device at various temperatures are shown in Fig. 3c. The area under the CV curves increases with increasing temperature, indicating improvement in charge storage capacity of the device. It was observed that the charge storage capacity of the device increases over 150 % by increasing temperature from 10 °C to 70 °C (Fig. 6S, ESI). The improved performance of the cobalt sulfide based supercapacitor device could be due to activation of the cobalt sulfide sites at higher temperature. In addition, the improvement could be due to and improved mobility of the electrolyte ions and lower series resistance at higher temperature.

The effect of temperature on the electrochemical behaviour of the supercapacitor was further investigated using electrochemical impedance spectroscopy (EIS). The variation of real and imaginary

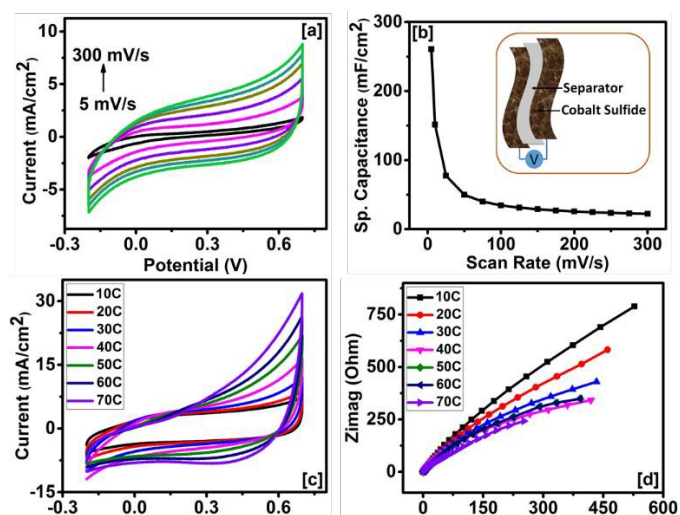


Fig. 3 (a) CV curves of supercapacitor device at various scan rate at room temperature, (b) variation of specific capacitance as a function of scan rate (inset figure show schematic diagram of the supercapacitor device), (c) CV curves of supercapacitor device at different temperature, and (d) Zreal vs. Zimag plots for the device at different temperature.

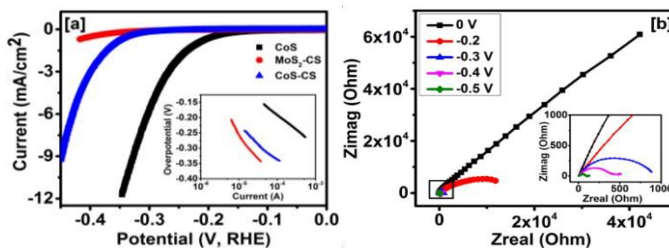


Fig. 4 (a) Polarization curves for synthesized cobalt sulfide (CoS), commercially samples of molybdenum sulfide (MoS₂-CS) and cobalt sulfide (CoS-CS) (inset figure show the Tafel plots) and (b) Zreal vs. Zimag plots at different potentials for cobalt sulfide.

impedance of the supercapacitor device at various temperatures is shown in Fig. 3d. The real and imaginary impedance of the device decreases with increasing temperature. The equivalent series resistance (ESR) of the supercapacitor device decreases with increasing temperature (Fig. 7S, ESI). The decrease in ESR with temperature could affect the charge storage properties of the device. The increase in the temperature enhances the mobility of the electrolyte ions and thus increases the conductivity of the electrolyte ions³⁵. The effect of temperature on the total impedance of the device is shown in Fig. 8S, ESI. It was observed that the impedance of the cobalt sulfide based supercapacitor device decreases with increasing temperature. The total impedance of the supercapacitor device was higher at lower frequency compared to that of at higher frequency. Our observations based on electrochemical characterizations suggest that the cobalt sulfide based supercapacitor device performs even better at elevated temperature than at room temperature.

The HER activity of the synthesized cobalt sulfide was also studied using glassy carbon working electrode with a standard rotating disk electrode instrument. All measurements were performed in 1N H₂SO₄ (aq) electrolyte under continuously purging with nitrogen gas (details in ESI). We have compared the HER activity of commercially available molybdenum sulfide (MoS₂-CS, Sigma, USA) and cobalt sulfide (CoS-CS, Strem Chemicals, USA) with our cobalt sulfide hollow structures. The polarization curves for the samples are shown in Fig. 4a. Cobalt sulfide showed a lower onset potential (0.21 V vs RHE) compare to MoS₂-CS (0.31 V vs RHE) and CoS-CS (0.35 V vs RHE). Our synthesized cobalt sulfide displayed about 60 and 30 times higher current density at 0.30 V (vs RHE) compared with MoS₂-CS and CoS-CS, respectively. The HER activity was further analysed using corresponding Tafel plots (inset of Fig. 4a). Tafel slope of 97 mV/decade, 174 mV/decade and 113 mV/decade was observed for synthesized cobalt sulfide, MoS₂-CS and CoS-CS, respectively. Lukowski *et al* have reported a Tafel slope of 112 mV/decade for as such synthesized nanostructured MoS₂³⁶. A Tafel slope of 75 mV/decade and 90 mV/decade was reported for CoS synthesized using microwave assisted and solvothermal methods, respectively³³. Sun *et al* have used electrodeposited cobalt-sulfide for HER application and reported a Tafel slope of 93 mV/s in phosphate buffer solution²⁶. CoS₂ synthesized using hydrothermal method showed a Tafel slope of 72 mV/s in acidic media³⁷. Peng *et al* have synthesized CoS₂/RGO/CNT nanocomposites for HER³⁸. A Tafel slope of about 51, 82 and 148 mV/s was observed for CoS₂/RGO/CNT, CoS₂/RGO and CoS₂, respectively. The rate of hydrogen evolution is limited either by proton adsorption onto an active site or evolution of the formed hydrogen from the surface. A high Tafel slope (120 mV/decade) is indicative of proton adsorption (Volmer step) as the rate-limiting step, while a lower Tafel slope (30 or 40 mV/decade)

COMMUNICATION

indicates that the evolution of molecular hydrogen from the catalyst is rate limiting (Heyrovsky or Tafel step, respectively). Tafel slope of 97 mV/decade for Co_{1-x}S suggest typical Volmer–Tafel route with the Volmer step as the rate determining step³⁹. Electrochemical impedance spectra of the cobalt sulfide were recorded at various potentials (Fig. 4b). As seen in the EIS spectra, the arc at zero potential converges to a semi-circle at negative potentials. A decrease in semi-circle diameter is observed with increase in negative potential. The charge-transfer resistance determined from the semicircle registered at low frequencies was found to be overpotential-dependent. Similar observation was reported for molybdenum phosphide⁹.

In conclusion, we have synthesized nanostructured cobalt sulfide by a facile hydrothermal method. The charge storage capacity and hydrogen evolution reaction activity were investigated using electrochemical methods. The highest specific capacitance of 867 F/g was observed at scan rate of 5 mV/s in cyclic voltammetry measurements. Cobalt sulfide showed a very stable electrochemical behaviour up to 5,000 cycles of charge-discharge study with highly flexible nature. The symmetrical supercapacitor device showed an areal capacitance of about 260 mF/cm² which improved over 150 % on raising the device temperature from 10 to 70 °C. The HER activity of cobalt sulfide was observed to be better than commercially available molybdenum sulfide. Our study suggests that cobalt sulfide could be used for high temperature operable flexible energy storage devices and an electrocatalyst for hydrogen evolution reaction.

Acknowledgements

Dr. Ram K. Gupta expresses his sincere acknowledgment to the Polymer Chemistry Initiative, Pittsburg State University for providing financial and research support. This material is partly based upon work supported by the National Science Foundation under Award No. EPS-0903806 and matching support from the State of Kansas through the Kansas Board of Regents. Dr. Ram K. Gupta acknowledges support from Department of Energy for Visiting Faculty Program. Authors thank Dr. Lifeng Dong for recording SEM/EDX. Drs. G. Gupta and A. Mohite thank Los Alamos LDRD.

Author contributions

RKG designed the experiments, run some structural and electrochemical characterization of the devices, interpret and analyze the data, and prepared the manuscript. CR, CZ, and EA helped in synthesis and performed some electrochemical characterizations. KR performed TEM measurement. GG and AM guided the hydrogen evolution studies. PK, PD, KR, BKG and GG reviewed the manuscript. All the authors reviewed and commented on the manuscript.

Additional information

The authors declare no competing financial interests. Requests for materials should be addressed to RKG.

References

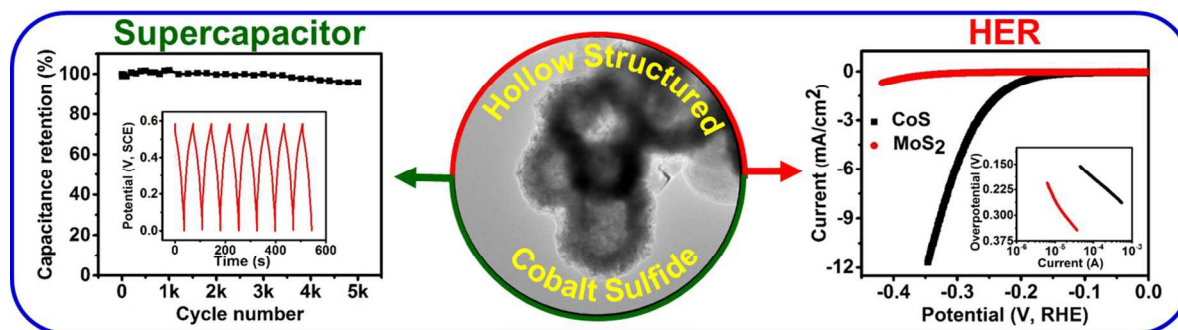
1. M. Winter and R. J. Brodd, *Chem. Rev.*, 2004, **104**, 4245-4270.
2. K. Ramasamy, R. K. Gupta, S. Palchoudhury, S. Ivanov and A. Gupta, *Chem. Mater.*, 2015, **27**, 379-386.
3. K. Ramasamy, H. Sims, W. H. Butler and A. Gupta, *J Am Chem Soc*, 2014, **136**, 1587-1598.
4. G. Wang, L. Zhang and J. Zhang, *Chem Soc Rev*, 2012, **41**, 797-828.
5. B. E. Conway, V. Birss and J. Wojtowicz, *J. Power Sources*, 1997, **66**, 1-14.
6. F. Zhao, Y. Wang, X. Xu, Y. Liu, R. Song, G. Lu and Y. Li, *ACS Applied Materials & Interfaces*, 2014, **6**, 11007-11012.
7. E. Mitchell, A. Jimenez, R. K. Gupta, B. K. Gupta, K. Ramasamy, M. Shahabuddin and S. R. Mishra, *New J. Chem.*, 2015, **39**, 2181-2187.
8. Y. Zhang, H. Feng, X. Wu, L. Wang, A. Zhang, T. Xia, H. Dong, X. Li and L. Zhang, *Int. J. Hydrogen Energy*, 2009, **34**, 4889-4899.
9. P. Xiao, M. A. Sk, L. Thia, X. Ge, R. J. Lim, J.-Y. Wang, K. H. Lim and X. Wang, *Energy & Environmental Science*, 2014, **7**, 2624-2629.
10. J. Deng, P. Ren, D. Deng, L. Yu, F. Yang and X. Bao, *Energy & Environmental Science*, 2014, **7**, 1919-1923.
11. M.-R. Gao, J.-X. Liang, Y.-R. Zheng, Y.-F. Xu, J. Jiang, Q. Gao, J. Li and S.-H. Yu, *Nat Commun*, 2015, **6**, 5982.
12. D. Voiry, H. Yamaguchi, J. Li, R. Silva, D. C. B. Alves, T. Fujita, M. Chen, T. Asefa, V. B. Shenoy, G. Eda and M. Chhowalla, *Nat Mater*, 2013, **12**, 850-855.
13. L. Cao, S. Yang, W. Gao, Z. Liu, Y. Gong, L. Ma, G. Shi, S. Lei, Y. Zhang, S. Zhang, R. Vajtai and P. M. Ajayan, *Small*, 2013, **9**, 2905-2910.
14. H. Yu, C. Zhu, K. Zhang, Y. Chen, C. Li, P. Gao, P. Yang and Q. Ouyang, *Journal of Materials Chemistry A*, 2014, **2**, 4551-4557.
15. W. Qiu, J. Xia, S. He, H. Xu, H. Zhong and L. Chen, *Electrochim. Acta*, 2014, **117**, 145-152.
16. X. Wang, J. Ding, S. Yao, X. Wu, Q. Feng, Z. Wang and B. Geng, *Journal of Materials Chemistry A*, 2014, **2**, 15958-15963.
17. J. M. Soon and K. P. Loh, *Electrochem. Solid-State Lett.*, 2007, **10**, A250-A254.
18. B. You and Y. Sun, *Advanced Energy Materials*, 2016, **6**, 1502333.
19. B. Sarma, R. S. Ray and M. Misra, *Mater. Lett.*, 2015, **139**, 77-80.
20. Y. Liu, W. Wang, H. Huang, L. Gu, Y. Wang and X. Peng, *Chem. Commun.*, 2014, **50**, 4485-4488.
21. S. Ratha and C. S. Rout, *ACS Applied Materials & Interfaces*, 2013, **5**, 11427-11433.
22. J. Yang, D. Voiry, S. J. Ahn, D. Kang, A. Y. Kim, M. Chhowalla and H. S. Shin, *Angewandte Chemie International Edition*, 2013, **52**, 13751-13754.
23. K.-J. Huang, J.-Z. Zhang, G.-W. Shi and Y.-M. Liu, *Mater. Lett.*, 2014, **131**, 45-48.
24. F. Tao, Y.-Q. Zhao, G.-Q. Zhang and H.-L. Li, *Electrochem. Commun.*, 2007, **9**, 1282-1287.
25. D. Kong, J. J. Cha, H. Wang, H. R. Lee and Y. Cui, *Energy & Environmental Science*, 2013, **6**, 3553-3558.
26. Y. Sun, C. Liu, D. C. Grauer, J. Yano, J. R. Long, P. Yang and C. J. Chang, *J Am Chem Soc*, 2013, **135**, 17699-17702.
27. M. S. Faber, M. A. Lukowski, Q. Ding, N. S. Kaiser and S. Jin, *The Journal of Physical Chemistry C*, 2014, **118**, 21347-21356.
28. Q. Wang, L. Jiao, H. Du, W. Peng, Y. Han, D. Song, Y. Si, Y. Wang and H. Yuan, *J. Mater. Chem.*, 2011, **21**, 327-329.
29. Q. Wang, L. Jiao, H. Du, Y. Si, Y. Wang and H. Yuan, *J. Mater. Chem.*, 2012, **22**, 21387-21391.

30. J.-C. Xing, Y.-L. Zhu, Q.-W. Zhou, X.-D. Zheng and Q.-J. Jiao, *Electrochim. Acta*, 2014, **136**, 550-556.
31. P. Justin and G. Ranga Rao, *Int. J. Hydrogen Energy*, 2010, **35**, 9709-9715.
32. R. S. Ray, B. Sarma, A. L. Jurovitzki and M. Misra, *Chem Eng J*, 2015, **260**, 671-683.
33. B. You, N. Jiang, M. Sheng and Y. Sun, *Chem. Commun.*, 2015, **51**, 4252-4255.
34. L. Zhang, H. B. Wu and X. W. Lou, *Chem. Commun.*, 2012, **48**, 6912-6914.
35. W. Li, K. Xu, L. An, F. Jiang, X. Zhou, J. Yang, Z. Chen, R. Zou and J. Hu, *Journal of Materials Chemistry A*, 2014, **2**, 1443-1447.
36. M. A. Lukowski, A. S. Daniel, F. Meng, A. Forticaux, L. Li and S. Jin, *J Am Chem Soc*, 2013, **135**, 10274-10277.
37. H. Zhang, Y. Li, G. Zhang, P. Wan, T. Xu, X. Wu and X. Sun, *Electrochim. Acta*, 2014, **148**, 170-174.
38. S. Peng, L. Li, X. Han, W. Sun, M. Srinivasan, S. G. Mhaisalkar, F. Cheng, Q. Yan, J. Chen and S. Ramakrishna, *Angewandte Chemie International Edition*, 2014, **53**, 12594-12599.
39. X. Zou and Y. Zhang, *Chem Soc Rev*, 2015, **44**, 5148-5180.

Graphical abstract

Highly stable hollow bifunctional cobalt sulfides for flexible supercapacitor and hydrogen evolution

C. Ranaveera^a, Z. Wang^a, E. Alqurashi^a, Bipin Kumar Gupta^b, Karthik Ramasamy^c, Aditya D. Mohite^d, Gautam Gupta^d and Ram K. Gupta^{*a}



Hollow structured cobalt sulfide exhibits excellent electrochemical properties for highly stable flexible supercapacitor and hydrogen evolution reaction (HER).